

Sliding Wear Response of a Bronze Bushing: Influence of Applied Load and Test Environment

B.K. Prasad

(Submitted June 23, 2011; in revised form January 3, 2012)

This investigation pertains to the examination of the sliding wear behavior of a leaded-tin bronze bushing under the conditions of varying applied loads and test environments against a steel shaft. The test environment was changed by adding 5% of solid lubricants like talc and lead to an oil lubricant separately as well as in combination; the fraction of the two (solid) lubricants within the solid lubricant mixture was varied in the range of 25–75% in the latter case. The wear performance of the bushing was characterized in terms of the wear rate, frictional heating, and friction coefficient. The increasing load led to deterioration in the wear response, while the addition of the solid lubricant particles produced a reverse effect. Further, an appreciable difference in the wear behavior was not observed when the tests were conducted in the oil plus talc and oil plus lead lubricant mixtures. However, the oil containing lead and talc together brought about a significant improvement in the wear response; best results were obtained in the case of the lubricant mixture consisting of lead and talc together in the ratio of 3:1 in the oil. The observed wear behavior of the samples has been discussed in terms of specific characteristics of various microconstituents. The features of the wear surfaces and subsurface regions further substantiated the wear response and enabled us to understand the operating material removal mechanisms.

Keywords journal bearing/bushing, leaded-tin bronze, lubricated wear, sliding wear behavior, solid lubricant

1. Introduction

Leaded-tin bronzes have widely been used in tribological applications including journal bearings (bushings) that encounter a sliding motion (Ref 1–7). Partially (mixed) lubricated conditions are usually encountered in such applications in view of the intermittent lubrication practice adopted (Ref 8). Mixed lubrication conditions are also encountered even during starting and stopping of fully lubricated sliding operations. Oil is an important class of lubricants used for such purposes. A number of additives are incorporated in the oil lubricants to improve the performance (Ref 8–10). Solid lubricants are one of the important additives in this context (Ref 8–21). Lead is a well-known solid lubricant (Ref 1, 2), while talc has been used to a very limited extent (Ref 22). The solid lubrication effect could be realized either through directly incorporating solid lubricating phases into the sliding material system (Ref 1, 2, 23–30) or by dispersing them in the base (liquid/ semi-solid) lubricant (Ref 8–21, 31–33) that subsequently goes in between the sliding surfaces. As far as the incorporation of lead into the sliding material systems is concerned, several examples exist in the literature (Ref 1, 2, 23–30), while very limited investigations have been carried out related to talc (Ref 4, 17–20, 22, 25).

The available information suggests that important parameters controlling the wear performance include the shape, size, content and nature of the solid lubricant phases in addition to other material and test related factors (Ref 11–21, 23–32). The nature of the dispersoid/matrix interface greatly controls the wear behavior. Also, since the solid lubricant phases are weak and soft in nature, their addition to the sliding material system leads to weakening the latter, thus causing deterioration in mechanical properties (Ref 34). It has also been noticed that their beneficial effects could be realized in this case in very specific sliding conditions only, with adverse effect being realized through the material chip off (Ref 23–30). Some information is also available with regard to the incorporation of the solid lubricants in oil (Ref 8–21, 31–33), wherein it has been observed that this mode of their use is free from the problems arising out of poor dispersoid/matrix interfacial characteristics and material weakening/chip off. Moreover, this mode of the solid lubricant addition offers the additive phase so as to directly and hence more effectively interact with the sliding surfaces, thus offering a better wear performance. Interestingly, most of the observations are based on the testing of standard samples like pins which offer a qualitative picture only pertaining to the wear behavior of materials (Ref 11–17, 19, 20, 23–32). Needless to say, observations drawn through component testing like journal bearings (bushings) become more realistic in nature and are one step nearer to practical applications.

In view of the above, an attempt has been made in this investigation to study the influence of incorporating lead and talc in a lubricating oil separately as well as in combination toward controlling the sliding wear response of a leaded-tin bronze journal bearing (bushing) at different applied loads. The features of wear surfaces and subsurface regions have also been examined to understand different operating wear mechanisms.

B.K. Prasad, CSIR-Advanced Materials and Processes Research Institute, Bhopal 462064, India. Contact e-mail: bkprasad@ampri.res.in.

Table 1 Chemical composition and hardness of the experimental bush and shaft

Material	Hardness (HV)	Chemical composition, wt.% element									
		Fe	C	Mn	Ni	Cr	Mo	Cu	Sn	Pb	Zn
Bronze Bush	84	(*)	5.14	5.22	4.75
Steel shaft	260	(*)	0.42	0.55	1.45	1.22	0.28

(*) remainder

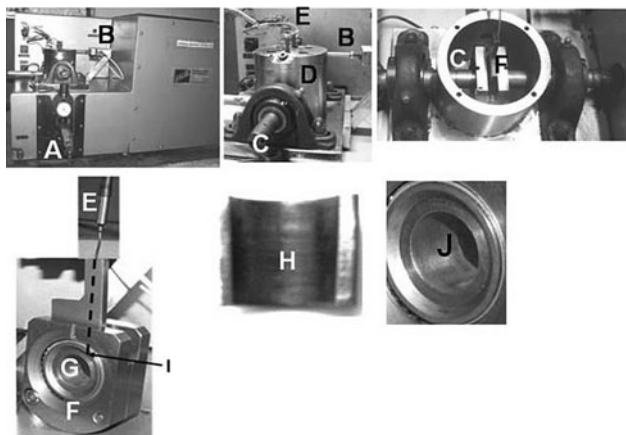


Fig. 1 Typical photographic views showing the journal bearing apparatus, inside the oil chamber, bearing housing with the bushing sample showing the position of the thermocouple and temperature measurement, and tested bush sample [A: cantilever mechanism, B: friction transducer, C: shaft, D: oil chamber, E: thermocouple, F: bearing housing, G: bushing sample, H: wear surface of the tested bushing, I: position of temperature measurement (outer surface of the bushing) and J: bushing sample before testing]

2. Experimental

2.1 Material and Sample Preparation

Cylindrical bushing samples (ID: 19.50 mm, OD: 25.4 mm, and length: 19.50 mm) were fabricated by machining. The starting material in this case was a leaded-tin bronze in the form of cylindrical rods (diameter: 28 mm and length: 150 mm) prepared by the liquid metallurgy route. The shaft was fabricated using En24 (conforming to SAE 4340) steel. Table 1 shows the chemical composition and hardness values of the bushing and shaft materials. The bushing and shaft were polished to a roughness (Ra) level of 0.25 μm .

2.2 Sliding Wear Tests

Lubricated sliding wear tests were performed on the bushing samples against the steel shaft. The test parameters used in this study were the sliding speed: 0.88 m/s, sliding distance: 1610 m, and applied loads: 300 and 400 lbs (corresponding to 136.08 and 182.44 kg, respectively). The wear test apparatus employed for the purpose was a Falex-make journal bearing tester. Figure 1 represents typical photographic views of the test apparatus and assembly and preworn, as well as tested bush samples. The composition of the test environment was varied by adding 5 wt% talc and lead (separately as well as in combination) to SAE40 oil lubricant; here the ‘%’ represents the weight of the solid lubricant

Table 2 Particle size, density and hardness of different solid lubricant particles mixed with the oil

Solid lubricant	Particle size range, μm	Density, g/cc	Hardness, Mohs	Melting point, $^{\circ}\text{C}$
Talc	25-100	2.58-2.83	1	1500
Lead	5-120	11.34	1.5	4327

particles in 100 cc of the oil lubricant. In the event of mixing the solid lubricant (lead and talc) particles together, the ratio of lead/talc was varied in the range of 0.33-3.0. Figure 2 shows the morphology of the talc and lead particles while Table 2 presents their particle size and properties. The lubricant mixture was stirred well before initiating the test. The shaft and bushing samples were cleaned well with acetone followed by carbon tetrachloride before and after testing. Weighing of the bushing was done using a Mettler microbalance having a precision level of 0.01 Mg. The wear rate was measured by the weight loss method. Frictional heat (generated at the outer surface of the bushing) and friction coefficient were recorded as a function of the test duration. For testing, the pre-weighed and cleaned bushing sample was fixed into the housing and the shaft inserted into the bushing. The lubricant mixture was filled in the chamber up to a level that allowed the shaft to get immersed up to its longitudinal axis. The bushing was loaded against the shaft with the help of a dead weight and a cantilever mechanism. The shaft was then rotated with the help of a drive mechanism at the predetermined sliding speed up to the specified distance.

2.3 Microscopic Studies

The microstructural analysis of the bronze (bushing) samples was carried out using optical and scanning electron microscopes. The samples were polished metallographically and etched with potassium dichromate solution. The worn-out part of the tested bush was cut for the study of the wear surfaces and subsurface regions. The transverse section of the cut piece was mounted in a polyester resin, polished according to the standard metallographic techniques and etched with potassium dichromate solution for the analysis of subsurface regions. Characteristics of the wear surfaces and subsurface regions were examined using scanning electron microscopy (SEM). The samples were mounted on brass studs and sputtered with gold before their SEM examination.

3. Results

3.1 Microstructure

Microstructural features of the bronze (bushing) sample are shown in Fig. 3. It shows a dendritic structure (Fig. 3a)

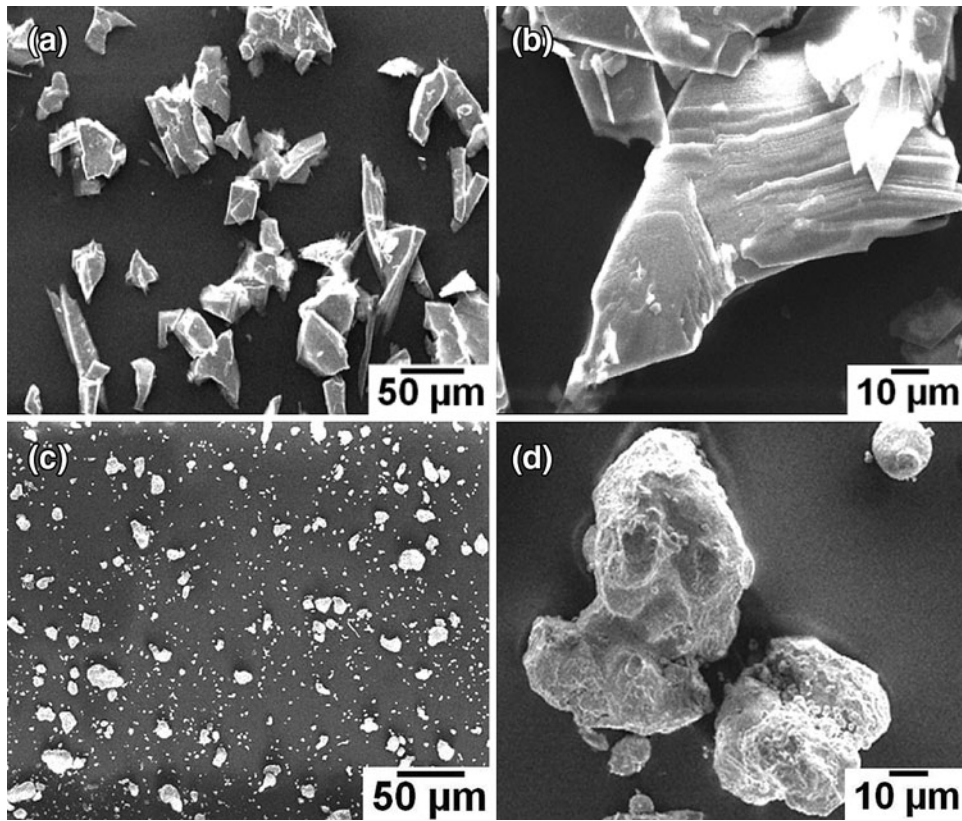


Fig. 2 Micrographs of (a and b) talc and (c and d) lead powder particles used as the solid lubricant in the oil lubricant mixture

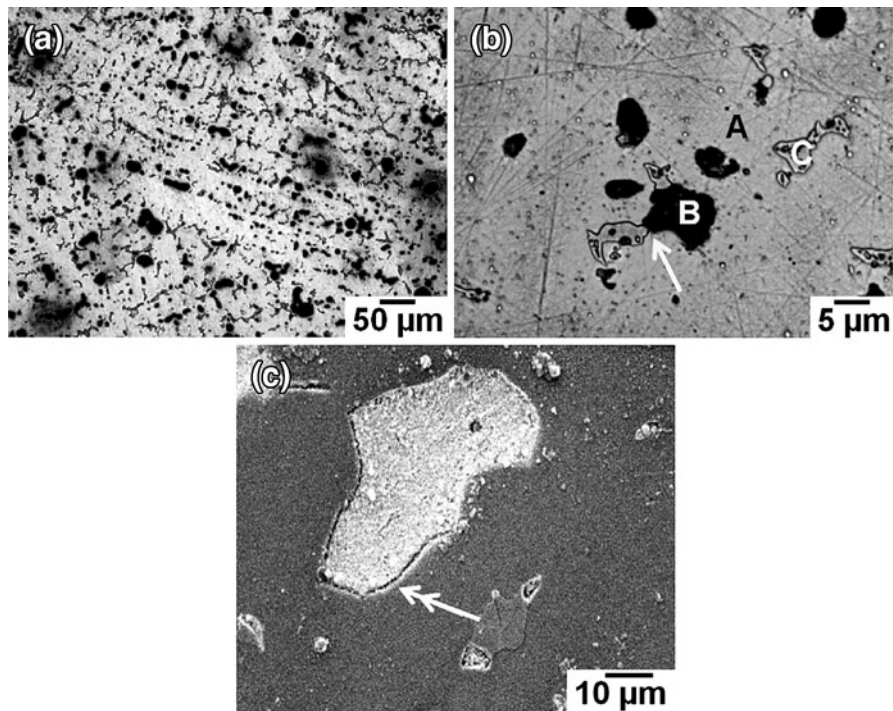


Fig. 3 Microstructural features of the bronze bushing sample showing (a) dendritic structure, (b) different phases and nucleation of lead at Cu-Sn intermetallic compound, and (c) occasional decohesion at lead/matrix interfacial regions [A: primary α , B: lead particle, C: copper-tin compound, single arrow: nucleation of lead at Cu-Sn compound and double arrow: decohesion]

comprising of primary α dendrites surrounded by the Cu-Sn intermetallic compound in the interdendritic regions and discrete particles of lead. A magnified view clearly reveals the presence of the α phase, lead particles, and Cu-Sn compound (Fig. 3b, regions marked by A, B, and C, respectively). A typical example of nucleation of lead particles on a

Cu-Sn compound is shown in Fig. 3(b) (the region marked by single arrow), while occasional decohesion of lead at the lead/matrix interface is evident in Fig. 3(c) (the region marked by double arrow).

3.2 Wear Behavior

Figure 4 shows the wear rate of the bushing samples at different applied loads. The influence of the test environment on the wear response of the samples is also evident from the figure. The wear rate increased with the load, while the presence of solid lubricant (talc and lead) particles in the oil produced a reverse effect. At the lower applied load, the wear performance of the samples was better when lead was mixed with the oil than that mixed with talc. However, the performance of lead and talc was comparable to each other at the higher test load. Interestingly, simultaneous mixing of both talc and lead with the oil was noted to be more effective toward reducing the wear rate of the samples wherein the degree of reduction in the wear rate became higher with the increasing fraction of lead in the lubricant mixture.

The temperature near the sliding surface of the bushing samples has been plotted as a function of the test duration in Fig. 5. The frictional heating increased with the test duration wherein the rate of increase was high initially followed by a lower rate of increase in the temperature—an exception being that, for the oil and oil + lead environments at the higher load (Fig. 5b), the highest rate of temperature increase was observed in the intermediate test duration. The presence of the solid lubricant particles in the oil lubricant led to a reduced severity of frictional heating in general. Also, the presence of talc and simultaneous addition of talc and lead to the oil caused the frictional heating to become the minimum.

The maximum temperature rise near the specimen surface is shown in Fig. 6 for each variable load. The influence of

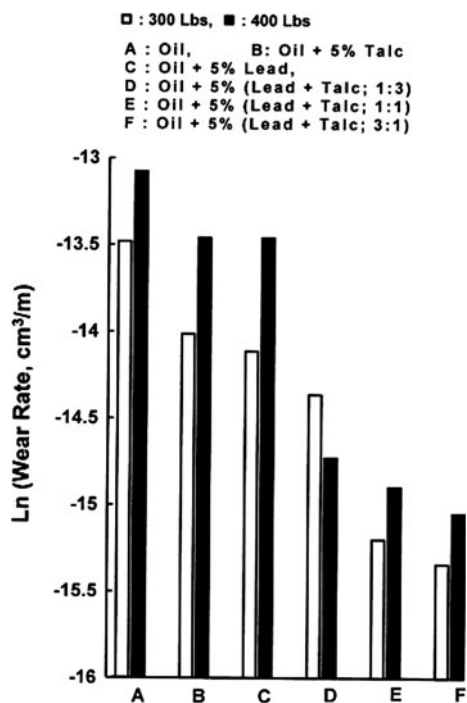


Fig. 4 Wear rate of the bushing samples for different combinations of solid lubricants mixed in the oil

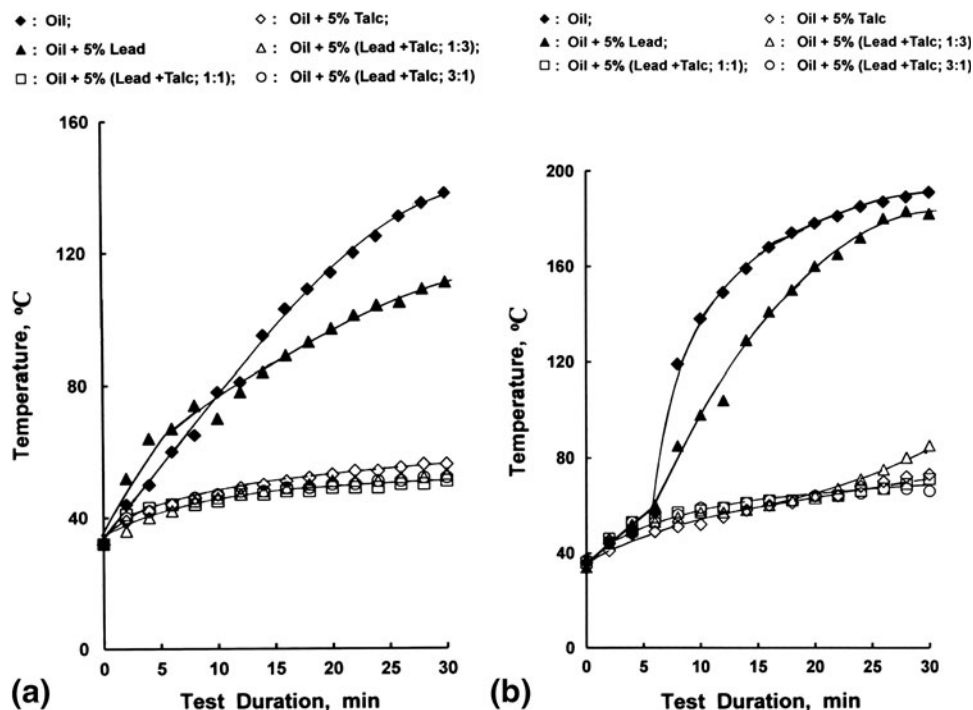


Fig. 5 Temperature near the surface of the bushing samples plotted as a function of test duration for different combinations of solid lubricants mixed with the oil lubricant at the applied load of (a) 300 lbs and (b) 400 lbs

changing the composition of the test environment is also evident from the figure. The increasing load led to a higher frictional heating. The severity of the frictional heating was

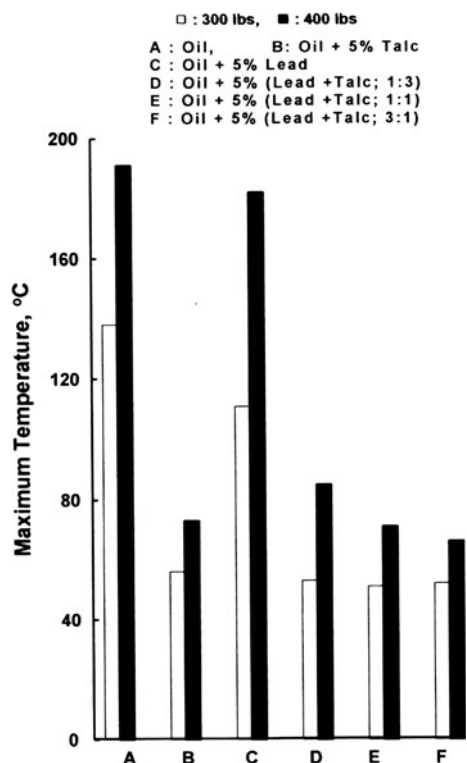


Fig. 6 Maximum temperature near the surface of the bushing samples at different applied loads for different combinations of solid lubricants mixed in the oil

comparable in the case of the oil and oil + lead lubricant mixtures, especially so at the higher applied load. Further, the simultaneous mixing of talc and lead particles with the oil lubricant brought about the least frictional heating, the extent of reduction in the temperature increasing with the rising fraction of lead in the lubricant mixture.

The curves for friction coefficient as a function of the test duration, in different environments have been plotted in Fig. 7. The friction coefficient was influenced by the test duration in a manner practically identical to that of the temperature (Fig. 5), excepting that the highest rate of increase in the friction coefficient was observed in the intermediate test duration even at the lower load (Fig. 7a). The influences of the load and test environment on the average friction coefficient (recorded toward the end of the tests) also were similar (Fig. 8) to that of the maximum temperature (Fig. 6).

3.3 Wear Surfaces

Figure 9 represents the wear surfaces of the bronze (bushing) samples. The wear surfaces generally showed the presence of well-defined grooves (Fig. 9a). Microcracks and deeper grooves were also observed (Fig. 9b, regions marked by single and double arrows, respectively). A magnified view clearly reveals the microcracking of the wear surface (Fig. 9c, regions marked by single arrow). Figure 9(d) represents a machining chip responsible for generating deeper wear grooves (the region marked by triple arrow). The exposure of a typical lead particle from within the bronze sample material is seen in Fig. 9(e) (the region marked by A). The presence of solid lubricant particles in the oil lubricant tended to produce in general smoother wear surfaces (Fig. 9f vs. a) along with the formation of a solid lubricant film (Fig. 9g, the region marked by B) to a greater extent.

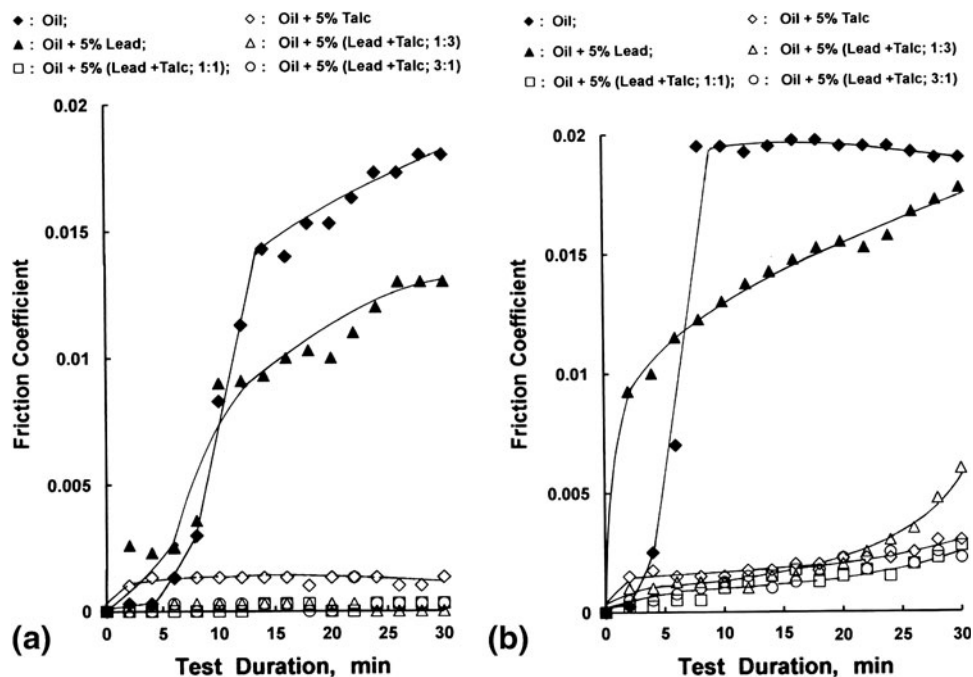


Fig. 7 Friction coefficient plotted as a function of test duration for different combinations of solid lubricants mixed with the oil lubricant at the applied load of (a) 300 lbs and (b) 400 lbs

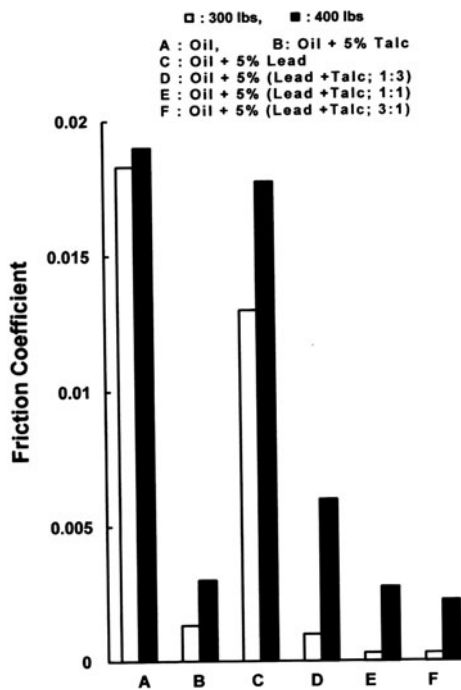


Fig. 8 Average friction coefficient at different applied loads for different combinations of solid lubricants mixed in the oil

3.4 Subsurface Regions

The features of the subsurface regions of the wear-tested samples are shown in Fig. 10. The flow of lead and other microconstituents in the sliding direction followed by the normal bulk structure was observed (Fig. 10a, regions marked by A and B, respectively). A magnified view (Fig. 10b) showed severe fragmentation of various microconstituents, microcracks (region marked by arrow), and regions in a process of separation from the bulk. The microcracks were observed to nucleate at the sharp tips of the microconstituents and propagate along the phase/matrix interfacial regions (Fig. 10c, the region marked by arrow).

4. Discussion

The bronze contained primary α , discrete particles of lead, and Cu-Sn compound (Fig. 3b, regions marked by A, B, and C, respectively). The α phase is soft and ductile and accommodates the hard Cu-Sn compound and soft lead particles. Being hard and strong, the Cu-Sn compound imparts load-bearing capability. The desired role of lead here is to act as a solid lubricant. However, the capability of lead toward producing the solid lubricating effect is solely controlled by the test parameters like the applied load, sliding speed, and environment (Ref 27, 28, 30). Broadly speaking, an optimum degree of frictional heat generation facilitates smearing of lead and subsequent adherence of the smeared mass on to the sliding surface. Conditions causing less frictional heating facilitate the predominant cracking tendency in the material, while the high frictional heat generation leads to material seizure leading to an inferior wear response in either case (Ref 27, 28, 30). The cracking tendency emanates from the nucleation of cracks from

the lead/matrix interface. The occasional decohesion observed in this study (Fig. 3c, the region marked by double arrow) further strengthens the view. The presence of sharp-tipped microconstituents enhances the tendency toward material cracking further (Fig. 10c, the region marked by arrow). Lead being soft and weak also produces weakening effect in the material system. Accordingly, addition of a solid lubricant phase to an external base lubricant (oil) always helps us to take care of the deterioration in the mechanical and wear properties of the material system, otherwise caused by the dispersion of the solid lubricant therein. Additional advantages of adding a solid lubricant phase to the external base lubricant include the availability of a better opportunity to smear on the sliding surfaces and form effective and stable lubricant film causing improved wear performance. The presence of oil imparts the film better adherence and stability on to the sliding surfaces by improving its wettability. The lubricating characteristic of a solid lubricant depends on properties like the hardness, structure, morphology, density, and quantity (Ref 11–21). Morphologies facilitating greater surface area are expected to improve the wear resistance. As far as the present study is concerned, lead is much heavier than that of graphite, while their particle size and hardness were comparable to each other (Table 2). From the point of view of structure, talc has a layered structure (Ref 35, 36), while that of lead is face centered cubic (Ref 37). Solids with the layered structure have very good smearing tendency along the layers, while the fcc structure allows the solids to deform easily in view of a large number of slip systems (number of close-packed planes multiplied by the number of close-packed directions). The simultaneous presence of both the kinds of solid lubricants on the sliding surfaces is expected to produce a synergistic effect in terms of improving the wear response of the samples.

The improvement in the wear response of the samples in the presence of the solid lubricant in the oil (Fig. 4) could be attributed to the formation of greater extent of lubricating film and its stability on the sliding surfaces (Fig. 9g, the region marked by B). Such layers reduce the severity and extent of direct metal-to-metal contact and hence better wear performance. The increasing concentration of lead in the lubricant mixture brought about improved response (Fig. 4). A corresponding reduction in frictional heating (Fig. 8) and friction coefficient (Fig. 6) was also in line with the decrease in the wear rate (Fig. 4). A comparison of the characteristics of talc and lead particles used in this study suggests significantly less density but relatively coarser particle size of talc compared to that of lead (Table 2). Also talc revealed layered structure (Fig. 2b), a feature that makes it more favorable as a solid lubricant, while lead does not possess such a feature (Fig. 2c and d). The lower density of talc suggests its greater volume fraction in the total lubricant mixture. Despite all the mentioned favorable features, the performance of talc was only comparable to that of lead (Fig. 4). This property indicates the overall influence of the size, density, and structure to neutralize the effects of each other on the overall wear response of the samples. Interestingly, however, the two solid lubricants i.e., lead and talc, despite displaying comparable performance in an identical manner, performed better when mixed together in varying proportions. One of the reasons could be that the relatively lighter and coarser particles of talc enable it to carry the finer and heavier lead particles (having a greater tendency toward settling) along, thus making the oil lubricant mixture more homogeneous in terms of the distribution of the

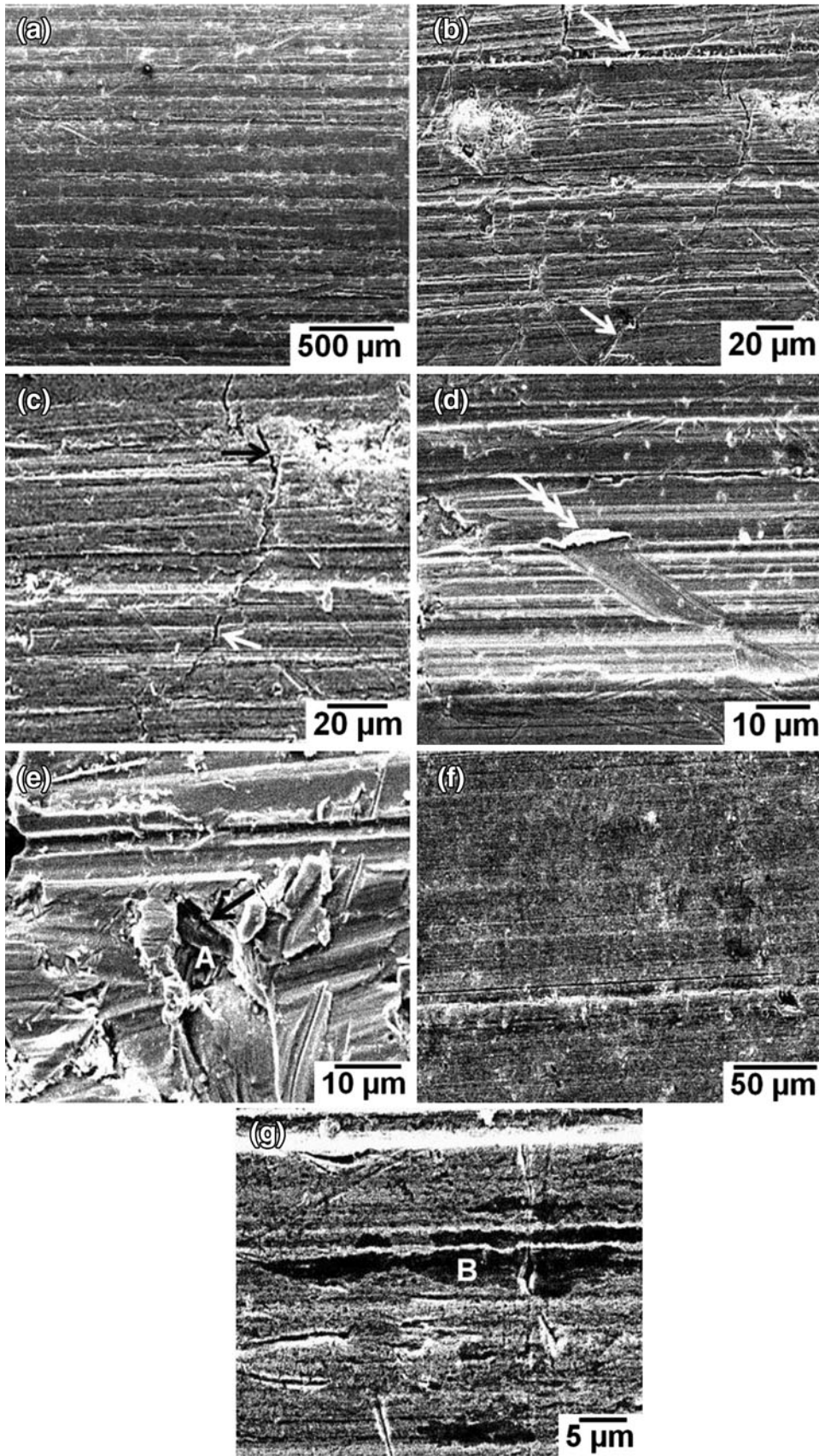


Fig. 9 Wear surfaces of the bushing samples tested in (a-e) oil, and (f and g) 5% lead + talc (3:1) at the applied load of 400 lbs [Single arrow: microcracks, double arrow: deep groove, triple arrow: machining chip entrapped in a deeper groove, A: exposure of lead and B: lubricating film formation]

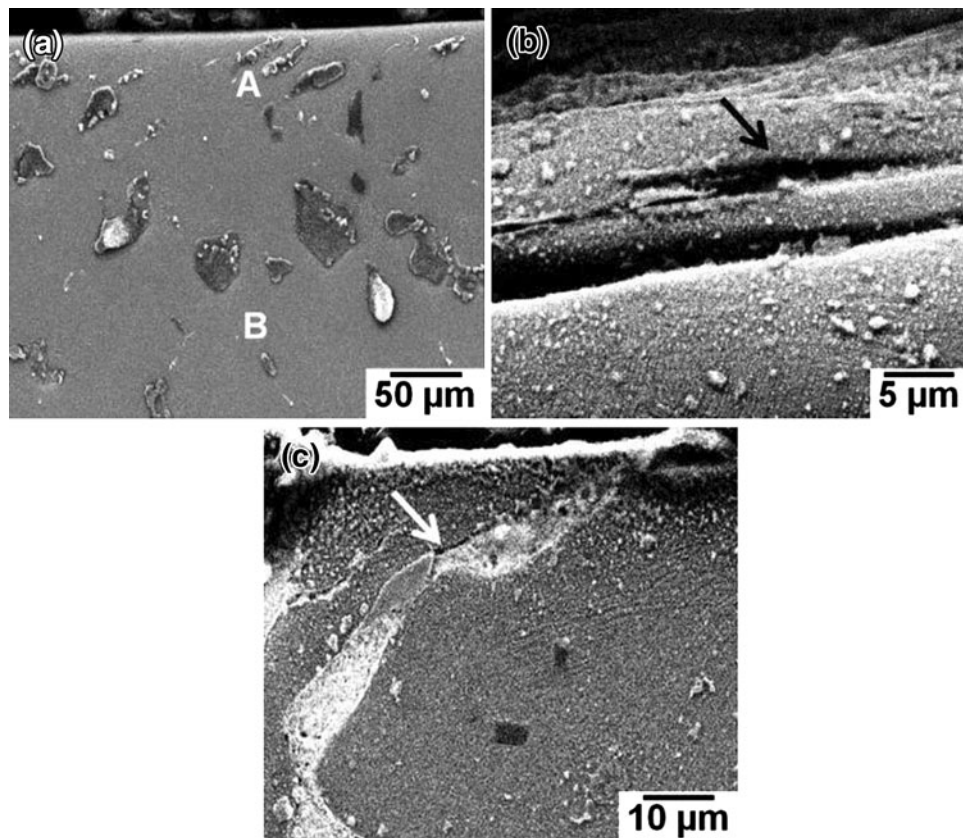


Fig. 10 Subsurface regions of the bronze bushing samples showing (a) flow of lead and other microconstituents in the sliding direction and (b and c) fragmentation of microconstituents along with cracking in the plastically deformed region [A: flow of microconstituents, B: unaffected bulk and arrow: crack]

suspended talc and lead particles, and hence offering improved wear performance.

The higher rate of increase initially observed in the frictional heating and friction coefficient with test duration (Fig. 5 and 7) is attributed to the abrasive action caused by the entrapment of the fragmented asperities that get work hardened due to severe wear-induced plastic deformation (Ref 38). It may be mentioned that the initially contacting asperities being significantly less in number have to carry the total effective load that exceeds their yield strength (Ref 39). This makes them to yield, work harden, and fragment in the due course of sliding. With the progress of the sliding process, the effective contacting surface area increases, as more and more of asperities establish contact with the counter surface. This makes the wear condition mild, and thus decreases the severity of frictional heating and friction coefficient at the longer test durations.

Deep grooves on the wear surfaces (Fig. 9b, the region marked by double arrow) are formed because of the hard debris that gets entrapped in between the sliding surfaces during the course of sliding (Fig. 9d, the region marked by triple arrow). The entrapped debris particles shown in the figure have been suggested to be generated through the scoring of the counterface (steel shaft in the present study) with hard microconstituents of the specimen material system (Ref 27, 28, 40). Cu-Sn intermetallic compound in the bronze bush (Fig. 3b, the region marked by C) could be a potentially responsible phase in this regard. The presence of cracks on the wear surfaces (Fig. 9c, the region marked by single arrow) emanates from the crack sensitive nature of leaded-tin bronzes in view of the presence of

lead particles in the material system. It has been suggested that lead is poorly soluble and exists as a mechanical mixture in the matrix (Ref 41, 42). Accordingly, the lead/matrix interface becomes a potential site for the crack nucleation and propagation as is evident from Fig. 9(e) and 10(c) (regions marked by single arrow). The occasional decohesion observed at the lead/matrix interface (Fig. 3c, the region marked by double arrow) further facilitates the process of cracking in the material.

The change in the degree of the wear-induced plastic deformation experienced by the regions at different depths below the wear surface (Ref 43, 44) is responsible for the variation in their microstructural features. Regions in the nearest vicinity of the wear surface undergo the highest severity of deformation leading to the generation of finest microconstituents (Fig. 10b). This is followed by the ones experiencing relatively a decreased severity of plastic deformation thus causing the microconstituents to flow in the sliding direction (Fig. 10a, the region marked by A). The unaffected region that was lying much below the surface (Fig. 10a, the region marked by B) revealed its features to be identical to that of the starting material (Fig. 3b).

Adhesion was noted to be the principal material removal mechanism. This was evident from the presence of plastically deformed regions on the wear surfaces (Fig. 9) and in the subsurface regions (Fig. 10). Microcracks on, as well as below, the wear surfaces (Fig. 9b and c and 10b and c, respectively) and decohesion at the lead/matrix interface (Fig. 3c, the region marked by double arrow) indicate that the interfacial regions serve as potential sites for the nucleation and propagation of microcracks, and the joining of such cracks result into material

removal during sliding. Entrapped hard (iron) debris particles on the wear surfaces (Fig. 9d, the region marked by triple arrow) causing deeper grooves on the wear surfaces delineate the contribution of abrasion also toward causing the material loss/degradation. The flow of lead particles (present within the bronze bush material system) in the sliding direction (Fig. 10a, the region marked by A) indicates the smearing tendency of the element toward forming the solid lubricating film (Fig. 9g, the region marked by B), while decohesion at the lead/matrix interface (Fig. 3c, the region marked by double arrow) shows its tendency to enhance cracking in the material system. Thus, the overall effect of lead depends on whether the cracking tendency or lubricating characteristics would be permitted by the test conditions to dominate. The talc and/or lead particles suspended in the oil lubricant also produce solid lubricating effect by smearing on the sliding surfaces.

5. Concluding Remarks

The present study suggests the wear response of the leaded-tin bronze bushing samples to improve in the presence of suspended talc and/or graphite particles. Interestingly, despite the comparable performance of talc and lead when mixed with oil separately, they delineated superior wear response when present in the lubricant mixture together. The improvement was observed in terms of reduced wear rate, frictional heating, and friction coefficient. Higher fraction of lead in the lubricant mixture in this case offered still improved wear characteristics of the bronze bushing. The frictional heating, friction coefficient, and wear rate became higher with the increasing load. Further, the frictional heating and friction coefficient increased at a higher rate with the increase in the test duration initially. This was followed by a reduced rate of the increase in the parameters at longer test durations. In some cases, the rates of increase in the frictional heating and friction coefficient were the highest in the intermediate test duration. The observed wear response of the samples was substantiated through the features of the wear surfaces. The wear surfaces were smoother in general at lower loads and in the presence of talc and/or lead in the oil that led to the improved wear performance and vice versa. The presence of the plastically deformed regions on the wear surfaces and below suggested adhesion to be an important wear mechanism. Further, the formation of dark patches/regions and entrapment and smearing of (lead/talc) particles on and below the wear surfaces suggested solid lubricating effect produced by the lead and talc particles. Formation of deep grooves and entrapped machining chips on the wear surfaces indicated abrasion also to play a role in causing the material removal. The decohesion at the lead/matrix interface and the presence of wear surface and subsurface cracks suggest that lead particles present within the (bronze) material system also tend to enhance the cracking tendency of the bronze, while producing the solid lubricating effect. In fact, the net influence of lead particles present within the bronze would depend on whether the sliding conditions permit the predominance of the cracking tendency or lubricating effect on each other.

References

- G.R. Kingsbury, Friction and Wear of Sliding Bearing Materials, *Metals Handbook: Friction, Lubrication and Wear Technology*, Vol 18, 10th ed., ASM, Materials Park, OH, USA, 1992, p 741–757
- G.C. Pratt, Materials for Plain Bearings, *Int. Metall. Rev.*, 1973, **18**, p 62–88
- R. Schouwenars, V.H. Jacobo, and A. Ortiz, Microstructural Aspects of Wear in Soft Tribological Alloys, *Wear*, 2007, **263**, p 727–735
- B.S. Ünlü, E. Atik, and C. Meriç, Effect of Loading Capacity (Pressure-Velocity) to Tribological Properties of CuSn10 Bearings, *Mater. Des.*, 2007, **28**, p 2160–2165
- T.S. Calayag, Zinc Alloys Replace Bronze in Mining Equipment Bushings and Bearings, *Mining Eng.*, 1983, **35**, p 727–728
- J.S. Rivas, J.J. Coronado, and A.L. Gómez, Tribological Aspects for the Shafts and Bearings of Sugar Cane Mills, *Wear*, 2006, **261**, p 779–784
- U. Ozsarac, F. Findik, and M. Durman, The Wear Behaviour Investigation of Sliding Bearings with a Designed Testing Machine, *Mater. Des.*, 2007, **28**, p 345–350
- B. Bhushan and B.K. Gupta, Solid Lubricants and Self-Lubricating Solids, Chapter 5, *Handbook of Tribology: Materials, Coatings and Surface Treatments*, McGraw Hill, New York, 1991, p 5.1–5.86
- R.H. Boehringer, Grease, *Metals Handbook: Friction, Lubrication and Wear Technology*, Vol 18, 10th ed., ASM, Materials Park, OH, USA, 1992, p 123–131
- W.O. Winer, Molybdenum Disulfide as a Lubricant: A Review of the Fundamental Knowledge, *Wear*, 1967, **10**, p 422–452
- B.K. Prasad, Effectiveness of an Externally Added Solid Lubricant on the Sliding Wear Response of a Zinc-Aluminium Alloy, Its Composite and Cast Iron, *Tribol. Lett.*, 2005, **18**, p 135–143
- B.K. Prasad, Sliding Wear Response of a Cast Iron Under Varying Test Environments and Traversal Speed and Pressure Conditions, *Wear*, 2006, **260**, p 1333–1341
- B.K. Prasad, Sliding Wear Response of Cast Iron as Influenced by Microstructural Features and Test Condition, *Mater. Sci. Eng. A*, 2007, **456A**, p 373–385
- B.K. Prasad and O.P. Modi, Sliding Wear Response of Zinc-Based Alloy as Affected by Suspended Solid Lubricant Particles in Oil Lubricant, *Tribol. Mater. Surf. Interfaces*, 2008, **2**, p 84–91
- B.K. Prasad, Sliding Wear Response of Spheroidal Graphite Cast Iron as Influenced by Applied Pressure, Sliding Speed and Test Environment, *Can. Metall. Q.*, 2008, **47**, p 495–507
- B.K. Prasad, Sliding Wear Behaviour of a Cast Iron as Affected by Test Environment and Applied Load, *Ind. Lubr. Tribol.*, 2009, **61**, p 161–172
- B.K. Prasad, S. Rathod, M.S. Yadav, and O.P. Modi, Effects of Some Solid Lubricants Suspended in Oil Towards Controlling the Wear Performance of a Cast Iron, *J. Tribol.*, 2010, **132**, p 1–9, Paper # 041602
- B.K. Prasad, S. Rathod, M.S. Yadav, and O.P. Modi, Influence of Talc Concentration in Oil Lubricant on the Wear Response of a Bronze Journal Bearing, *Wear*, 2010, **269**, p 498–505
- B.K. Prasad, S. Rathod, M.S. Yadav, and O.P. Modi, Wear Behaviour of Cast Iron: Influence of MoS₂ and Graphite Addition to the Oil Lubricant, *J. Mater. Eng. Perf.*, 2011, **20**, p 445–455
- B.K. Prasad, Influence of Suspended Talc Particles in Oil and Nature of Material Microconstituents on Sliding Wear Characteristics of Cast Iron and Zinc-Based Alloy, *Can. Metall. Q.*, 2009, **48**, p 455–464
- B.K. Prasad, S. Rathod, M.S. Yadav, and O.P. Modi, The Influence of Lead Suspension in Oil Lubricant on the Sliding Wear Behaviour of Cast Iron, *Tribol. Lett.*, 2010, **37**, p 289–299
- J. Ribet, K. Poret, D. Arsequel, D. Chulia, and F. Rodriguez, Talc Functionality as Lubricant: Texture, Mean Diameter and Specific Area Influence, *Drug Dev. Ind. Pharm.*, 2003, **29**, p 1127–1135
- P.K. Rohatgi, Y. Liu and S. Ray, Friction and Wear of Metal Matrix Composites, *Metals Handbook: Friction, Lubrication and Wear Technology*, Vol 18, 10th ed., ASM, Materials Park, OH, USA, 1992, p 801–811
- P.K. Rohatgi, S. Ray, and Y. Liu, Tribological Properties of Metal Matrix-Graphite Particle Composites, *Int. Mater. Rev.*, 1992, **37**, p 129–152
- A.K. Jha, T.K. Dan, S.V. Prasad, and P.K. Rohatgi, Aluminium Alloy-Solid Lubricant Talc Particle Composites, *J. Mater. Sci.*, 1986, **21**, p 3681–3685
- Y. Tsuya, H. Shimura, and K. Umeda, A Study of the Properties of Copper and Copper-Tin Base Self-Lubricating Composites, *Wear*, 1972, **22**, p 143–162
- B.K. Prasad, A.K. Patwardhan, and A.H. Yegneswaran, Factors Controlling the Dry Sliding Wear Behaviour of a Leaded-Tin Bronze, *Mater. Sci. Technol.*, 1996, **12**, p 427–435

28. B.K. Prasad, A.K. Patwardhan, and A.H. Yegneswaran, Wear Characteristics of a Zinc-Based Alloy Compared with a Conventional Bearing Bronze under Mixed Lubrication Condition: Effects of Material and Test Parameters, *Can. Metall. Q.*, 2001, **40**, p 193–210
29. B.K. Prasad, Sliding Wear Response of a Gray Cast Iron: Effects of Some Experimental Parameters, *Tribol. Int.*, 2011, **44**, p 660–667
30. B.K. Prasad, Sliding Wear Behaviour of Bronzes Under Varying Material Composition, Microstructure and Test Conditions, *Wear*, 2004, **257**, p 110–123
31. F. Wilson and T.S. Eyre, Addition of Graphite Particles to Oil Lubricants, *Lubr. Eng.*, 1973, **29**, p 65–72
32. M. Yazun, Z. Wancheng, L. Shengna, J. Yuansheng, W. Yuscong, and T.C. Simon, Tribological Performance of Three Advanced Piston Rings in the Presence of MoDTC-Modified GF-3 Oils, *Tribol. Lett.*, 2005, **18**, p 75–83
33. S.Q.A. Rizvi, Lubricant Additives and Their Functions, *Metals Handbook: Friction, Lubrication and Wear Technology*, Vol 18, 10th ed., ASM, Materials Park, OH, USA, 1992, p 98–112
34. B.S. Mazumder, A.H. Yegneswaran, and P.K. Rohatgi, Strength and Fracture Behaviour of Metal Matrix Particulate Composites, *Mater. Sci. Eng. A.*, 1984, **68**, p 85–96
35. P.K.D. Poddar and M. Chaudhuri, Chapter 2, Natural Minerals, *Handbook of Ceramics*, S. Kumar, Ed., Kumar and Associates Publishers, Calcutta, 1994, p 53–104
36. J.A. Radosta and N.C. Trivedi, Talc, *Handbook of Fillers and Reinforcements for Plastics*, H.S. Kartz and V. Milewski, Ed., Van Nostrand Reinhold Publishers, New York, 1978, p 160–171
37. E.A. Brandes, *Smithells Metals Reference Book*, 6th ed., Butterworth and Co., London, 1983, p 370–801
38. D.A. Rigney, L.H. Chen, M.G.S. Naylor, and A.R. Rosenfield, Wear Processes in Sliding Systems, *Wear*, 1984, **100**, p 195–219
39. F.E. Kennedy, Jr., Thermal and Thermomechanical Effects in Dry Sliding, *Wear*, 1984, **100**, p 453–476
40. O.P. Modi, B.K. Prasad, A.H. Yegneswaran, and M.L. Vaidya, Dry Sliding Wear Behaviour of Squeeze Cast Aluminium Alloy-Silicon Carbide Composites, *Mater. Sci. Eng. A*, 1992, **151A**, p 235–245
41. J.P. Pathak and S.N. Tiwari, On the Mechanical and Wear Properties of Copper-Lead Alloys, *Wear*, 1992, **155**, p 37–47
42. W.A. Glaeser, Transfer of Lead from Leaded Bronze During Sliding Contact, *Proceedings of International Conference on Wear of Materials*, Vol 2, Denver, USA, April 1989, ASME, p 255–260
43. O. Yilmaz and H. Turhan, Effect of Size and Volume Fraction of Particulates on the Sliding Wear Resistance of CuSn Composites, *Wear*, 2001, **249**, p 901–913
44. Z. Shi, Y. Sun, A. Bloyce, and T. Bell, Unlubricated Rolling-Sliding Wear Mechanisms of Complex Aluminium Bronze Against Steel, *Wear*, 1996, **193**, p 235–241